Available online at www.sciencedirect.com

SciVerse ScienceDirect

Ceramics International 39 (2013) S659–S662

CERAMICS INTERNATIONAL

www.elsevier.com/locate/ceramint

Performance of anode-supported solid oxide fuel cell in planar-cell channel-type setup

Hyung-Tae Lim[a,b,*], Soon Cheol Hwang[b], Jin Soo Ahn[b]

[a]School of Nano & Advanced Materials Engineering, Changwon National University, Changwon, Gyeongnam 641-773, Republic of Korea
[b]Fuel Cell Project, Research Institute of Industrial Science and Technology (RIST), Pohang, Gyeongbuk 790-600, Republic of Korea

Available online 17 October 2012

Abstract

In a planar-cell channel-type setup, the electrochemical performance of a solid oxide fuel cell strongly depends on the operating conditions. In this study, a large-area (10×10 cm^2) anode-supported solid oxide fuel cell was fabricated and tested in a single cell stack. It was found that the gas conversion overpotential can be significant depending on the fuel utilization, and this additional overpotential is not related to the electrode's electrochemical performance. Thus, the gas conversion overpotential must be taken into account for accurate analysis of the electrochemical performance of an SOFC stack, particularly under high fuel utilization conditions.

Keywords: E. Fuel cells; C. Impedance; Gas conversion

1. Introduction

There are many factors limiting the electrochemical performance of solid oxide fuel cells (SOFCs) on the level of a large area stack that are usually not detected on the level of a button cell. One of these factors is the gas conversion overpotential, which is defined as the effect of current passing through electrodes at a finite gas flow rate [1]. When an anode-supported button cell is tested with a good conducting contact layer such as a Pt or Ag mesh and a sufficient fuel gas supply to minimize contact resistance and gas conversion polarization, the cell components and their factors responsible for voltage losses are as follows [2]: (1) ohmic resistance dominated by the resistivity and thicknesses of the electrolyte and electrodes, (2) activation polarization (charge transfer resistance) dominated by the electrode microstructure (three-phase boundaries) and gas composition, and (3) concentration polarization dominated by the electrodes' microstructures (pore sizes and thicknesses) and gas composition. Regarding voltage loss factors at the stack level, the testing setup for a planar cell with a large area is quite different from that for a button-sized cell. Metallic interconnectors (bipolar plates) used in a stack can cause a significant contact resistance that changes the current distribution depending on the rib design [3,4]. The type of current collector (material and geometry) should also be carefully chosen because it plays an important role in the electrochemical performance of an SOFC stack [5]. In the case of an oxygen-ion conducting electrolyte-based fuel cell, hydrogen fuel is consumed and water is produced at the anode side by an electrochemical reaction. Consequently, the gas concentration at the electrolyte/anode interface changes, indicating that gas concentration polarization is established across the anode layer. In anode-supported cells, this polarization effect due to limited gas diffusion through the porous anode is considerable. In a button cell test, the test geometry is typically simple, and the fuel gas supply is usually sufficient for the active area (because fuel utilization is not the main concern) so that the gas concentration polarization is mainly governed by gas diffusion through the porous anode support layer rather than gas conversion over the anode support layer. In large-area anode-supported cells (in a fuel cell stack), gas-phase transport has a large impact on the SOFC performance [1,6–9]. In particular, in

*Corresponding author at: School of Nano & Advanced Materials Engineering, Changwon National University, Changwon, Gyeongnam 641-773, Republic of Korea.
E-mail address: htaelim@changwon.ac.kr (H.-T. Lim).

0272-8842/$ - see front matter © 2012 Elsevier Ltd and Techna Group S.r.l. All rights reserved.
http://dx.doi.org/10.1016/j.ceramint.2012.10.156

the case of planar cells, the fuel gas flows along the anode gas channel length, parallel to the anode surface at a finite gas flow rate so that concentration gradients are established from the gas inlet to the outlet region because of fuel depletion [6,9]. Consequently, it is not expected that the electrochemical reaction will occur evenly throughout the active area of the cell. Thus, the problem of how to enhance the gas exchange between the hydrogen and water above the anode in order to minimize the concentration gradient should be considered. If the fuel cell stack is operated under high fuel utilization (low gas flow rate), gas exchange is not very effective, resulting in a concentration change above the surface of the anode (Nernst loss), i.e., increase in gas conversion overpotential, which is usually not observed in the button cell test setup where the fuel gas stream is perpendicular to the cell surface. The voltage losses in a fuel cell stack can be formulated as

$$E(i) = E_{\mathrm{OCV}} - (\eta_{\Omega} + \eta_{\alpha} + \eta_{\delta} + \eta_{\mu} + \eta_{\upsilon}) \quad (1)$$

where $E(i)$, E_{OCV}, η_{Ω}, η_{α}, η_{δ}, η_{μ} and η_{υ} are the cell voltage under operation, open circuit voltage, ohmic voltage drop, activation overpotential, voltage drop due to gas diffusion in electrodes, voltage drop due to gas cross-over across electrolyte, and voltage drop due to gas conversion (gas conversion overpotential), respectively [8]. Let us focus on the anode gas conversion overpotential, which can be written as [1]

$$\eta_{\upsilon,a} = \frac{RT}{2F}\left(\ln\left(\frac{x_{i,\mathrm{H_2}}}{x_{i,\mathrm{H_2O}}}\right) + \ln\left(\frac{x_{i,\mathrm{H_2O}} + i/J_i 2F}{x_{i,\mathrm{H_2}} - i/J_i 2F}\right)\right) \quad (2)$$

where $\eta_{\upsilon,a}$ is the anodic gas conversion overpotential, R is the gas constant, T is the absolute temperature, F is Faraday's constant, J_i is the inlet area-specific gas flow rate (mol/cm^2 s), and i is the current density. $x_{i,\mathrm{H_2O}}$ and $x_{i,\mathrm{H_2}}$ are the inlet mole fractions of water and hydrogen, respectively. For a low current range, Eq. (1) reduces to

$$\eta_{\upsilon,a} = \frac{RT}{4F^2 J_i}\left(\frac{1}{x_{i,\mathrm{H_2O}}} + \frac{1}{x_{i,\mathrm{H_2}}}\right) i \quad (3)$$

Eqs. (1) and (2) imply that the gas conversion overpotential can be depressed by a high flow rate J_i, which enhances the gas exchange over the anode. The above equations also show that the gas conversion overpotential strongly depends on the operating conditions such as fuel gas composition, flow rate, and temperature. In this study, the anode-supported SOFC was tested in a planar-cell channel-type setup as a function of the gas flow rate (fuel utilization) and channel geometry (cross-sectional area) in order to understand how the performance of a single cell stack is limited by the gas conversion overpotential.

2. Experimental procedure

The anode-supported cells were fabricated with an area of 100 cm^2, and the active (cathode) area was 81 cm^2. The anode support layer, NiO+YSZ (yttira stabilized zirconia) of ~900 μm; the functional layer, NiO+YSZ of ~15 μm; and the electrolyte layer, YSZ of ~10 μm were tape-casted and then laminated and co-sintered at ~1300 °C. After sintering, the buffer layer, GDC (gadolinia doped ceria) of 1–2 μm was aerosol-deposited to prevent the formation of an insulating layer between the YSZ and LSCF layers. The cathode functional layer, LSCF (lanthanum strontium cobalt ferrite peroskite)+GDC of ~15 μm and cathode current collector, LSCF of ~40 μm were screen-printed and then fired at ~1000 °C. For the single stack test setup, Fe–Cr alloy end plates were machined for the co-flow of fuel and oxidant gases through internal manifolds and gas channels with dimensions of 1000 μm (width) × 250 μm (depth). Humidified hydrogen fuel (3%) was supplied in a range of flow rates of 1–6 LPM, which was controlled by using a mass flow controller (Brooks Instruments). For the oxidant gas at the cathode, air was supplied at a fixed flow rate of 2.5 LPM. In order to investigate the influence of the cross-sectional area of the gas channel, three different gas channel geometries were prepared: (1) 1000 (width) × 250 (depth) μm^2, (2) 1000 (width) × 600 (depth) μm^2, and (3) no channel. In the third case, the fuel gas was transported only through the pores of the Ni foam. A schematic of the single cell stack configuration with the gas channels is shown in Fig. 1. Impedance and current-voltage (I–V) curve measurements were conducted as functions of the gas flow rate (fuel utilization) and cross-sectional area of the gas channel at 750 °C.

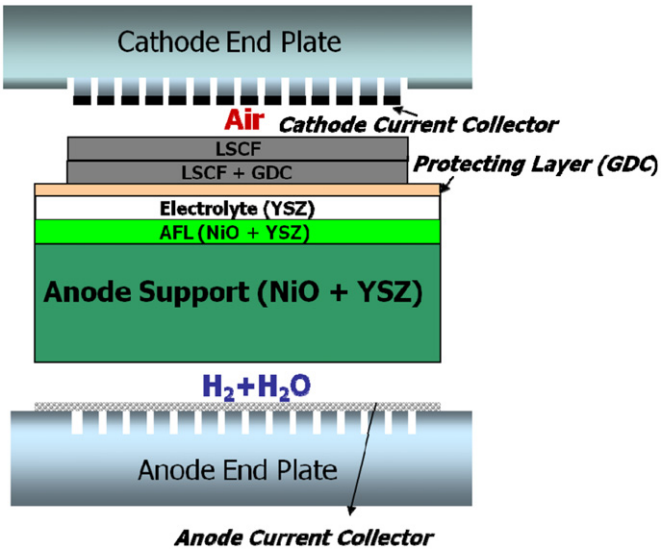

Fig. 1. A schematic of the single cell stack design for this study.

3. Results and discussion

Fig. 2 shows the effect of the fuel gas flow rate on the impedance, particularly on the second semi-circle of the impedance at low frequencies (< 0.1 Hz). As the gas flow rate decreased from 6 LPM (liter per minute) to 1 LPM (increasing the fuel utilization from 6 to 25%), the second arc significantly increased; in particular, the impedance at the very low frequency range (0.1–0.01 Hz) was significantly

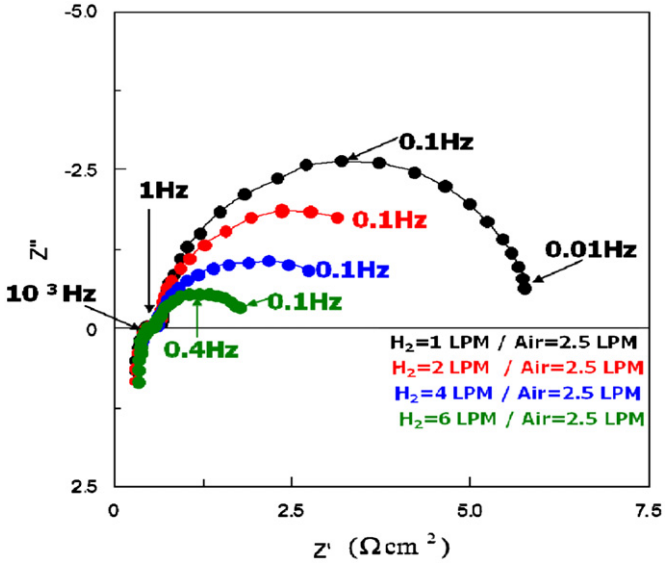

Fig. 2. Impedance spectra over at circuit as a function of fuel flow rate.

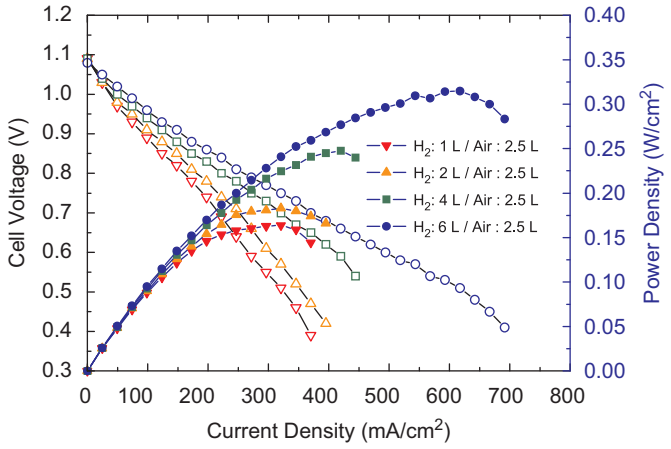

Fig. 3. A plot of the cell I–V curve as a function of fuel flow rate.

increased. At a gas flow rate of 6 LPM, the intercept of the second arc on the real axis was at ~0.1 Hz. However, as the flow rate decreased, the second arc was not completed at 0.1 Hz, but was extended to the lower frequency of ~0.01 Hz. In other words, the additional impedance between 0.1 and 0.01 Hz was developed with a decrease in the flow rate. It should be noted that the first semicircle at high frequencies of 10^3~1 Hz (dominated by activation polarization resistance) did not change much. Thus, the additional impedance of 0.1–0.01 Hz is believed to be due to gas conversion since it was depressed simply by the fuel gas flow rate. At a gas flow rate of 6 LPM, the impedance in the range of 0.1–0.01 Hz disappeared, and thus, it can be said that the second arc in the range of 1–0.1 Hz was dominated by only concentration polarization due to gas diffusion through the porous electrodes. In contrast, at gas flow rates below 6 LPM, the second arc was dominated by the gas conversion above the anode's surface as well as the gas diffusion through the anode; as the gas flow rate decreased, the gas conversion became more dominant.

The corresponding I–V measurements as a function of the fuel flow rate are shown in Fig. 3. As observed in the impedance measurements, the I–V characteristics (power density) of the single cell stack were also improved by increasing the flow rate, which means that the gas exchange over the anode became more effective and the gas conversion overpotential was eliminated in the high flow rate. In other words, as sufficient fuel gas was supplied to the anode side, the hydrogen concentration in the fuel stream could be maintained without Nernst loss. The calculated gas conversion overpotentials using Eqs. (2) and (3) are shown in Fig. 4(a) and (b), respectively. Here, T is 750 °C, hydrogen is 3% humidified ($x_{i,H_2O} = 0.03$, $x_{i,H_2} = 0.97$), and J_i is 1 LPM (~9.24×10^{-6} mol/cm² s) and 6 LPM (~1.54×10^{-6} mol/cm² s) for 91 cm². These conditions are typical gas compositions and flow rates for a 100-cm² planar cell test. It should be noted that, as shown in Fig. 4(a), the area specific resistance due to gas conversion (slope of the plot) is high at low currents and high currents, while it is low at medium currents. Let us compare this calculated data with the results of the I–V curve as a function of the flow rate in Fig. 3.

In Fig. 3, if the gas conversion overpotential is assumed to be zero at a gas flow rate of 6 LPM, the voltage drop by decreasing the flow rate from 6 LPM to 1 LPM is attributed to the gas conversion overpotential. At a current density of ~0.3 A/cm² (practical current density for fuel cell stack), the voltage difference between 1 LPM and 6 LPM is ~0.22 V. From Eqs. (2) and (3), it is found that the overpotential differences between 1 LPM and 6 LPM are ~0.06 V and ~0.21 V, respectively. Because the applied current density is ~0.3 A/cm², which is in the low current region, the gas conversion overpotential calculated using Eq. (3) agrees well with the measured overpotential rather than with the general equation, i.e., Eq. (2). Thus, it can be said that the voltage loss in the single cell stack due to the low flow rate (high fuel utilization) is related to the gas conversion above the anode's surface (in the gas channel), and not to the electrochemistry of the anode itself. In other words, the performance of the fuel cell stack is significantly affected not only by the electrochemical properties of the stack components but also by the testing conditions such as fuel utilization.

Bessler et al. numerically studied the effects of the gas channel geometry on the gas conversion overpotential [6]. They showed that the resistance due to gas conversion decreases with an increase in the cross-sectional area in the channel diffusion model while remaining constant in the case of the channel flow model. We experimentally conducted a performance test (I–V characteristics) of a single cell stack as a function of the channel cross-sectional area. Fig. 5 compares the results of the I–V curve measurements at 750 °C among the gas channels with depths of 200 μm, 600 μm, and 0 μm. The fuel flow rate was constant at 6 LPM. There was no significant difference in the I–V

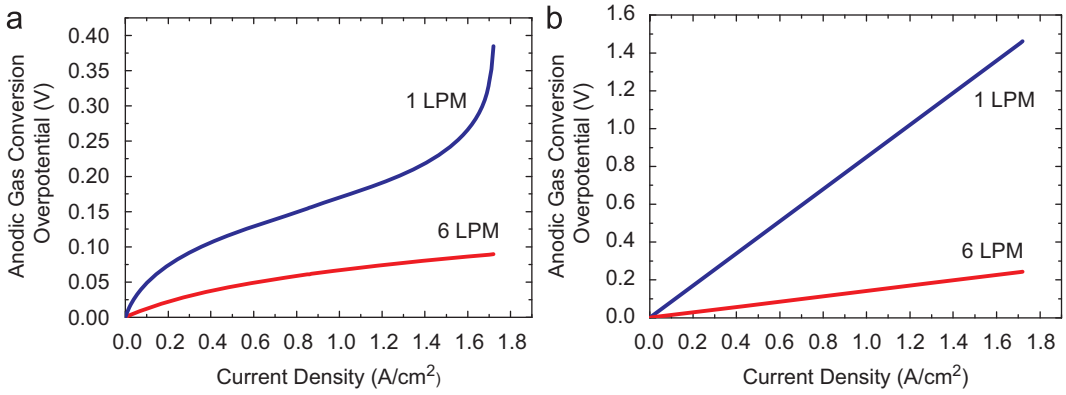

Fig. 4. A plot of anodic gas conversion overpotential calculated using (a) Eq. (2) and (b) Eq. (3).

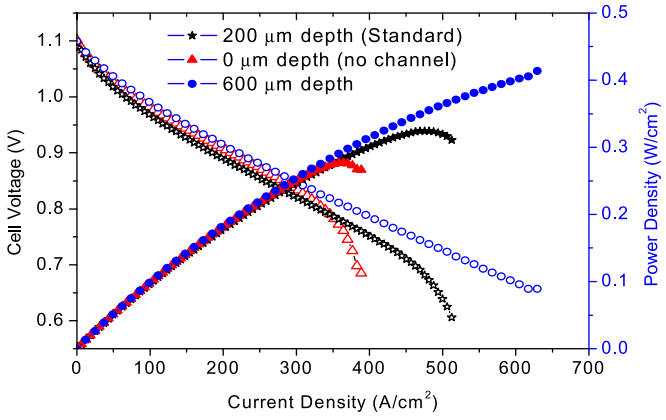

Fig. 5. A plot of the cell I–V curve as a function of channel geometry.

curve in the range of 0–350 mA/cm^2; however, the limiting current density increased with the cross-sectional area. It should be noted that the cells used for each test were fabricated from the same batch; thus, the electrochemical performance of each cell can be assumed to be essentially the same. In addition, the other components such as the anode and cathode current collectors were all identical for each test. Thus, the reason for the improved I–V characteristics in the high current region should be related to the gas channel depth. On the other hand, our experimental data in the low current region agrees with Bessler's channel flow model (constant resistance versus cross-sectional area). Unfortunately, it is not fully understood why the performance of the single cell stack is a function of the channel geometry only in the high current region. This mechanism will be studied further in future work.

4. Conclusion

The gas overpotential can be depressed by increasing the fuel flow rate, i.e., enhancing the effective gas exchange over the anode. It is important to distinguish this additional overpotential due to operating conditions such as gas flow rate and gas composition from the other polarization phenomenon caused by the electrochemical performance of the anode itself. Thus, gas conversion overpotential must be considered for analysis of the electrochemical performance of a large-area anode-supported SOFC in a planar-cell channel-type setup. Particularly when fuel utilization (stack efficiency) is the main concern for commercialization, efforts should be made to create an efficient gas supply design to enhance the gas exchange over the anode, i.e., to decrease the gas conversion overpotential.

Acknowledgments

This research was supported by research funds of POSCO and Basic Science Research Program through the National Research Foundation of Korea (NRF), funded by the Ministry of Education, Science and Technology (2012013782).

References

[1] S. Primdahl, M. Mogensen, Gas Conversion Impedance, Journal of the Electrochemical Society 145 (7) (1998) 2431–2438.
[2] S.C. Singhal, K. Kendall, High temperature solid oxide fuel cells, Elsevier, 2004.
[3] S. Liu, C. Song, Z. Lin, The effect of the interconnect rib contact resistance on the performance of planar solid oxide fuel cell stack and the rib design optimization, Journal of Power Sources 183 (2008) 214–225.
[4] M. Kornely, A. Leonide, A. Weber, E. Ivers-Tiffee, Performance limiting factors in anode-supported originating from metallic interconnector design, Journal of Power Sources 196 (2011) 7209–7216.
[5] S.P. Jiang, J.G. Love, L. Apateanu, Effect of contact between electrode and current collector on the performance of solid oxide fuel cells, Solid State Ionics 160 (2003) 15–26.
[6] W.G. Bessler, S. Gewies, Gas concentration impedance of solid oxide fuel cell anodes II, Journal of the Electrochemical Society 154 (6) (2007) B548–B559.
[7] T. Jacobsen, P.V. Hendriksen, S. Koch, Diffusion and conversion impedance in solid oxide fuel cells, Electrochimica Acta 53 (2008) 7500–7508.
[8] M.-P. Heddrich, L. Dorrer, R.-U. Dietrich, G. Borchardt, Chr. Arigiusis, A simple model for prediction of polarization loss phenomena in a SOFC stack, ECS Transactions 7 (1) (2007) 1987–1993.
[9] H.-T. Lim, S. Hwang, Y. Park, I. Lee, Performance and long term stability of large area anode supported solid oxide fuel cells, solid state ionics 225 (2012) 124–130.